

Detection of Higher Order Modulation Harmonics in Magnetic
Resonance Force Microscopy

T. Mewes – University of Alabama

et al.

Deposited 08/28/2018

Citation of published version:

Mewes, T., et al. (2007): Detection of Higher Order Modulation Harmonics in Magnetic Resonance Force Microscopy, *Journal of Applied Physics*, 102(3). <https://doi.org/10.1063/1.2761779>

Detection of higher order modulation harmonics in magnetic resonance force microscopy

T. Mewes, C. K. A. Mewes, E. Nazaretski, J. Kim, K. C. Fong, Y. Obukhov, D. V. Pelekhov, P. E. Wigen, and P. C. Hammel

Citation: [Journal of Applied Physics](#) **102**, 033911 (2007); doi: 10.1063/1.2761779

View online: <https://doi.org/10.1063/1.2761779>

View Table of Contents: <http://aip.scitation.org/toc/jap/102/3>

Published by the [American Institute of Physics](#)

Articles you may be interested in

[The design and verification of MuMax3](#)

[AIP Advances](#) **4**, 107133 (2014); 10.1063/1.4899186

[Study of structural and ferromagnetic resonance properties of spinel lithium ferrite \(LiFe₅O₈\) single crystals](#)

[Journal of Applied Physics](#) **117**, 233907 (2015); 10.1063/1.4922778

[Precise determination of the spectroscopic g-factor by use of broadband ferromagnetic resonance spectroscopy](#)

[Journal of Applied Physics](#) **114**, 243906 (2013); 10.1063/1.4852415

[Spin torque switching of perpendicular Ta|CoFeB|MgO-based magnetic tunnel junctions](#)

[Applied Physics Letters](#) **98**, 022501 (2011); 10.1063/1.3536482

[Ferromagnetic resonance force microscopy on a thin permalloy film](#)

[Applied Physics Letters](#) **90**, 234105 (2007); 10.1063/1.2747171

[Perpendicular magnetic anisotropy in Pd/Co thin film layered structures](#)

[Applied Physics Letters](#) **47**, 178 (1985); 10.1063/1.96254

Detection of higher order modulation harmonics in magnetic resonance force microscopy

T. Mewes^{a)} and C. K. A. Mewes

*Center for Materials for Information Technology/Department of Physics and Astronomy,
University of Alabama, Box 870209 Tuscaloosa, Alabama 35487*

E. Nazaretski

Los Alamos National Laboratory, MPA-10, Los Alamos, New Mexico 87545

J. Kim, K. C. Fong, Y. Obukhov, D. V. Pelekhov, P. E. Wigen, and P. C. Hammel

Department of Physics, Ohio State University, 191 West Woodruff Avenue, Columbus, Ohio 43210

(Received 30 April 2007; accepted 13 June 2007; published online 6 August 2007)

Magnetic resonance force microscopy measurements of the electron spin resonance of a thin film of 2,2-diphenyl-1-picrylhydrazyl were performed using a low doped silicon cantilever with a high coercivity SmCo particle glued to its end. The low doping level enables amplitude modulation of the microwave field with only small spurious driving of the cantilever. Besides amplitude modulation we use frequency modulation of the microwave field at integer fractions of the cantilever resonance frequency leading to derivative signals up to the fourth derivative of the amplitude modulation response signal. The influence of the modulation depth on the line shape of the first derivative response is also presented. © 2007 American Institute of Physics. [DOI: [10.1063/1.2761779](https://doi.org/10.1063/1.2761779)]

I. INTRODUCTION

Magnetic resonance force microscopy (MRFM) is a scanning probe technique based on mechanical detection of the magnetic resonance signal¹ due to the magnetic interaction between a high-gradient probe micromagnet mounted on a compliant micromechanical cantilever and the magnetic moments in the sample under investigation. The strength of this interaction is measured through detection of the cantilever displacement. To improve sensitivity of the method, magnetic moments in the sample are selectively manipulated using a magnetic resonance technique in such a manner that the force of magnetic probe-sample interaction is modulated at a frequency equal to the mechanical resonance frequency of the cantilever. This approach allows taking advantage of the high quality factor Q of the mechanical cantilever. The MRFM technique has demonstrated sensitivity much greater than that of conventional inductive and cavity based methods of magnetic resonance detection. MRFM has been successfully used for detection of nuclear magnetic resonance,^{2,3} ferromagnetic resonance,^{4,5} and electron spin resonance (ESR),^{6,7} recently demonstrating single spin sensitivity.⁸ This unprecedented sensitivity, combined with a capability for selective manipulation of spins in the sample makes MRFM a valuable tool for spatially resolved magnetic resonance detection and subsurface three-dimensional magnetic resonance imaging.

One common problem of MRFM experiments is the so called spurious coupling or modulation noise,^{9–12} i.e., the undesired excitation of the sensing cantilever through forces other than those originating from the magnetic resonance signal one is interested in. This is especially pronounced in the case when the electromagnetic field amplitude is modu-

lated at the mechanical resonance frequency of the cantilever ω_0 . One common solution to this problem is to modulate the microwave frequency^{12,13} rather than the amplitude of the microwave field at the cantilever frequency. Another solution is to use an anharmonic modulation scheme,⁹ for which two quantities are modulated simultaneously. The modulation frequencies are chosen such that their sum or difference matches the resonance frequency ω_0 of the cantilever. Typical implementations of this anharmonic modulation scheme use the modulation of the static magnetic field together with amplitude modulation of the microwave field⁹ or mechanical modulation of the sample magnetization together with modulation of the static magnetic field.¹⁴ As another solution to the modulation noise problem the usage of poorly conducting cantilevers has been proposed.¹²

In the present article we demonstrate that the use of low doped silicon cantilevers enables amplitude modulation of the microwave field with negligible spurious coupling to the cantilever. We furthermore extend the frequency modulation scheme previously used to frequency modulation at integer fractions of the cantilever frequency thereby enabling detection of higher order derivatives of the magnetic resonance signal.

II. EXPERIMENT

In a typical magnetic resonance force microscopy experiment the inhomogeneous field of a microscopic magnetic particle attached to the end of a cantilever is used to locally excite electron spin resonance in a sample. The region of the sample in which the resonance condition

^{a)}Electronic mail: tmewes@ua.edu

$$|\mathbf{B}_{\text{tot}}(\mathbf{r})| = \frac{\omega}{\gamma} \quad (1)$$

is met is often called the sensitive slice. Here $\mathbf{B}_{\text{tot}}(\mathbf{r}) = \mathbf{B} + \mathbf{B}_{\text{tip}}(\mathbf{r})$ is the total magnetic field at the position \mathbf{r} in the sample and consists of the (homogenous) external magnetic field \mathbf{B} and the tip field $\mathbf{B}_{\text{tip}}(\mathbf{r})$. The magnetic resonance in the sample is excited with a microwave field with frequency ω and γ denotes the gyromagnetic ratio. Besides localizing the magnetic resonance in the sample the inhomogeneous tip field also couples the sample magnetization $\mathbf{m}(\mathbf{r}, t)$ to the mechanical resonator. The total force \mathbf{F}_{tot} acting on the cantilever is given by¹⁵

$$\mathbf{F}_{\text{tot}}(t) = \int_{\text{sample}} dV \mathbf{F}(\mathbf{r}, t), \quad (2)$$

where $\mathbf{F}(\mathbf{r}, t)$ is the force originating from a point \mathbf{r} in the sample and is given by

$$\mathbf{F}(\mathbf{r}, t) = -[\mathbf{m}(\mathbf{r}, t) \cdot \nabla] \mathbf{B}_{\text{tip}}(\mathbf{r}). \quad (3)$$

Whenever this force has a sufficiently large Fourier component at the cantilever resonance frequency ω_0 the large Q factor of the cantilever (in our experiments: $Q \approx 200\,000$, measured using a ring-down experiment)¹⁶ will lead to a detectable oscillation amplitude of the cantilever. By using an interferometric detection scheme for the cantilever displacement,¹⁷ even at 4 K the sensitivity of a magnetic resonance force microscope is limited by the thermal motion of the cantilever itself. The Fourier component of the force at the cantilever frequency can be generated, for example, by amplitude modulation of the microwave excitation at the cantilever frequency or by frequency modulation of the microwave frequency either at the cantilever frequency or at integer fractions of the cantilever frequency. The details of the expected spectra together with experimental results obtained from a thin film of 2,2-diphenyl-1-picrylhydrazyl (DPPH) measured at 4 K will be discussed in the following. The details of the experimental setup and the cantilever to

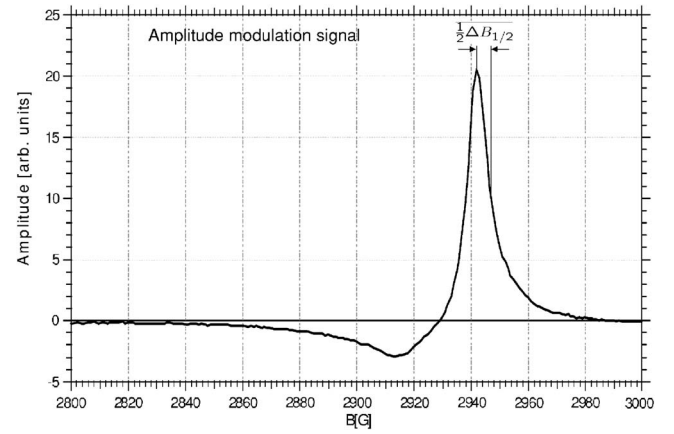


FIG. 1. Cantilever amplitude signal as a function of the externally applied magnetic field. The microwave field (8.29 GHz) was amplitude modulated at the cantilever frequency and the signal was detected using a lock-in amplifier at the same frequency.

which we glued a SmCo particle (magnetic tip) and shaped it using focused ion beam have been described elsewhere.⁵

A. Amplitude modulation

One approach to generating a significant driving force at the resonance frequency of the cantilever is to modulate the amplitude H_1 of the radio frequency field

$$H_1^{\text{AM}}(t) = H_1^0(1 + \xi \cos \omega_m t), \quad (4)$$

where $0 \leq \xi \leq 1$ is the modulation depth and $\omega_m = \omega_0$ is the modulation frequency chosen to be equal to the cantilever frequency. A detailed description of the probe sample coupling and the expected response for amplitude modulation can be found in Ref. 15. A typical spectrum obtained from DPPH at 4 K (see Fig. 1) clearly shows the expected features: at low fields the resonance condition is only fulfilled for spins located in a narrow shell underneath the tip, the sensitive slice. For external magnetic field within the intrinsic linewidth ΔB_0 of the resonance field, i.e., for $|B - \omega/\gamma| < \Delta B_0$, all parts of the sample for which the tip field is neg-

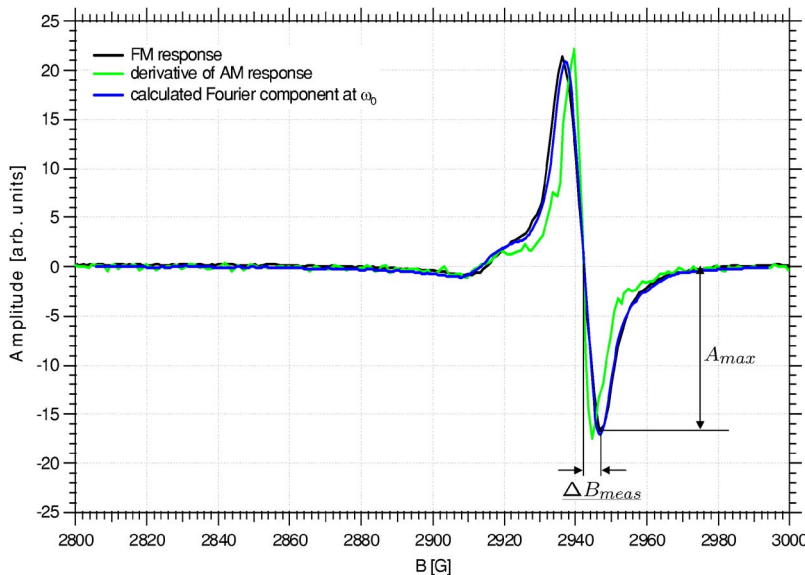


FIG. 2. (Color online) Cantilever amplitude as a function of the applied magnetic field. Here the microwave field was frequency modulated with a modulation amplitude of $\Delta\omega/\gamma = 5.4$ G at the cantilever frequency, the signal at the same frequency was detected using a lock-in amplifier. The black line shows the experimental data, the green line is the numerical derivative of the data shown in Fig. 1, while the blue line is obtained from the same data by calculating the Fourier component at ω_0 .

ligible are at resonance. The sign change of the tip field gradient between the sample regions underneath the tip and far away from the tip is the origin of the sign change of the force acting on the cantilever, which leads to the characteristic MRFM-line shape as observed in Fig. 1. One common drawback of using amplitude modulation is the fact that this scheme usually generates large spurious forces acting on the cantilever. As pointed out for example by Suter¹² using a poorly conducting material for the cantilever should reduce this effect. Therefore, in our experiments we used a low boron doped ($\approx 10^{15} \text{ cm}^{-3}$) Si cantilever. As can be seen in Fig. 1 this leads to a very small spurious coupling to amplitude modulation, i.e., a negligible offset of the entire spectrum with respect to the zero base line.

B. Frequency modulation at the cantilever frequency

In the case of frequency modulation^{13,18} (FM) the frequency ω of the microwave excitation is modulated about its average frequency $\bar{\omega}$,

$$\omega(t) = \bar{\omega} + \Delta\omega \cos(\omega_m t). \quad (5)$$

Here $\Delta\omega$ denotes the frequency modulation depth and ω_m is the modulation frequency. For the following discussion we

assume that $1/T_1 \gg \omega_m/2\pi$, which implies that for time scales of the order of $1/\omega_m$ the magnetization is always in equilibrium. Here T_1 denotes the longitudinal relaxation time. The resonance condition (1) in the case of frequency modulation reads

$$|\mathbf{B}_{\text{tot}}| = \frac{\bar{\omega}}{\gamma} + \frac{\Delta\omega}{\gamma} \cos(\omega_m t). \quad (6)$$

Thus frequency modulation can also be thought of as a field modulation¹⁹⁻²¹ around the average field $\bar{B} = \bar{\omega}/\gamma$ with a modulation $\Delta B(t) = (\Delta\omega/\gamma)\cos(\omega_m t)$. Assuming that the field dependence of the force $F(B)$ acting on the cantilever is known one can perform a Taylor-series expansion around \bar{B} ,

$$\begin{aligned} F(\bar{B} + \Delta B) &= \sum_{m=0}^{\infty} \frac{1}{m!} \left. \frac{\partial^m F}{\partial B^m} \right|_{\bar{B}} (\Delta B)^m \\ &= \sum_{m=0}^{\infty} \frac{1}{m!} \left. \frac{\partial^m F}{\partial B^m} \right|_{\bar{B}} \left[\frac{\Delta\omega}{\gamma} \cos(\omega_m t) \right]^m. \end{aligned} \quad (7)$$

This expansion can be rewritten in a Fourier-series expansion in $\cos(m\omega_m t)$ as follows:

$$\begin{aligned} m=0: & F(\bar{B}), \\ m=1: & \left. \frac{\partial F}{\partial B} \right|_{\bar{B}} \frac{\Delta\omega}{\gamma} \cos(\omega_m t), \\ m=2: & \frac{1}{2} \left. \frac{\partial^2 F}{\partial B^2} \right|_{\bar{B}} \left[\frac{\Delta\omega}{\gamma} \cos(\omega_m t) \right]^2 = \frac{1}{4} \left. \frac{\partial^2 F}{\partial B^2} \right|_{\bar{B}} \frac{\Delta\omega^2}{\gamma^2} [1 + \cos(2\omega_m t)], \\ m=3: & \frac{1}{6} \left. \frac{\partial^3 F}{\partial B^3} \right|_{\bar{B}} \left[\frac{\Delta\omega}{\gamma} \cos(\omega_m t) \right]^3 = \frac{1}{24} \left. \frac{\partial^3 F}{\partial B^3} \right|_{\bar{B}} \frac{\Delta\omega^3}{\gamma^3} [3 \cos(\omega_m t) + \cos(3\omega_m t)], \\ m=4: & \frac{1}{24} \left. \frac{\partial^4 F}{\partial B^4} \right|_{\bar{B}} \left[\frac{\Delta\omega}{\gamma} \cos(\omega_m t) \right]^4 = \frac{1}{192} \left. \frac{\partial^4 F}{\partial B^4} \right|_{\bar{B}} \frac{\Delta\omega^4}{\gamma^4} [3 + 4 \cos(2\omega_m t) + \cos(4\omega_m t)], \\ m=5: & \frac{1}{120} \left. \frac{\partial^5 F}{\partial B^5} \right|_{\bar{B}} \left[\frac{\Delta\omega}{\gamma} \cos(\omega_m t) \right]^5 = \frac{1}{1920} \left. \frac{\partial^5 F}{\partial B^5} \right|_{\bar{B}} \frac{\Delta\omega^5}{\gamma^5} [10 \cos(\omega_m t) + 5 \cos(3\omega_m t) + \cos(5\omega_m t)]. \end{aligned} \quad (8)$$

Thus by modulating the microwave frequency at the cantilever frequency, i.e., $\omega_m = \omega_0$, the Fourier component at the cantilever frequency reads

$$\left[\left. \frac{\partial F}{\partial B} \right|_{\bar{B}} \frac{\Delta\omega}{\gamma} + \frac{1}{8} \left. \frac{\partial^3 F}{\partial B^3} \right|_{\bar{B}} \frac{\Delta\omega^3}{\gamma^3} + \mathcal{O}(\Delta\omega^5) \right] \cos(\omega_0 t). \quad (9)$$

So to first order in $\Delta\omega$ the response is

$$\left(\left. \frac{\partial F}{\partial B} \right|_{\bar{B}} \frac{\Delta\omega}{\gamma} \right) \cos(\omega_0 t). \quad (10)$$

Therefore, for small modulation depths $\Delta\omega$ the frequency modulation response is proportional to the derivative of the amplitude modulation response,^{18,22,23} as can be seen in Fig. 2. One notices that the apparent linewidth of the measured frequency modulation response is larger than the one obtained using amplitude modulation. This is caused by the

rather large modulation amplitude of $\Delta\omega/\gamma=5.4$ G used in this case.

While the expression in Eq. (10) is a good approximation for small modulation depths and any line shape the experimentally observed frequency modulation response can be calculated for any field modulation depth $\Delta B_m = \Delta\omega/\gamma$ numerically for any given field dependence of the force $F(B)$ acting on the cantilever as follows: The time dependence of the force during frequency modulation is simply given by the time dependence of the total magnetic field $F_{FM}(t) = F(|\mathbf{B}_{tot}(t)|)$. If either the line shape of the sample is known analytically or the amplitude response is measured experimentally one can calculate this force numerically over a full modulation cycle and by performing a Fourier transform of this force $\mathcal{F}(F_{FM})$ one obtains the frequency spectrum of the force at multiples of the modulation frequency. In Fig. 2 the Fourier component at ω_0 calculated based on the measured amplitude response (compare Fig. 1) is shown for the experimental parameters used in this case. The curve agrees better than the estimate based on Eq. (10), as this approach is, at least for an analytically known line shape, valid for arbitrary modulation depths. Using the experimentally measured amplitude response to calculate the force spectrum is, however, only advisable as long as the field separation of those data points is significantly smaller than the field modulation depth for which the frequency modulation response is to be predicted. The noise present in the experimental data further limits the applicability of this approach.

From measurements of the frequency modulation response of the sample at different modulation depths ΔB_m , the measured half linewidth ΔB_{meas} and the signal amplitude A_{max} were determined as shown in Fig. 2. Note that we have used the half linewidth rather than the full linewidth, which one would measure between the maximum and minimum of the FM response, in order to minimize the influence of the localized resonance underneath the tip. The results are shown in Figs. 3(a) and 3(b), respectively. In these graphs the expected linewidth and signal amplitude have been calculated based on the numerical scheme described earlier assuming both a Lorentzian and a Gaussian line shape with a full width at half maximum (FWHM) of 9.2 and 6.2 G, respectively, which for both line shapes corresponds to the measured half linewidth of $\Delta B_0 = 2.7$ G for small modulation depths. The FWHM $\Delta B_{1/2} = 9$ G determined directly from the amplitude modulation data in Fig. 1 is in better agreement with a Lorentzian line shape. The measured linewidth dependence on the modulation depth is similar for both line shapes. However, the signal amplitude seems to be better described by a Gaussian line shape, compare Fig. 3(b). As is well known, there is an optimum modulation depth which results in a maximum signal^{24,25} which can be seen in our numerical simulations for the Gaussian line as well as in the experimental data. For the Lorentzian line shape the maximum signal amplitude will occur at modulation depths larger than is observed experimentally.²⁵ The measured signal amplitude drops off faster than one would expect for either a Lorentzian or Gaussian line shape. Thus we conclude that while simple analytical line shapes can provide useful guidance to the ac-

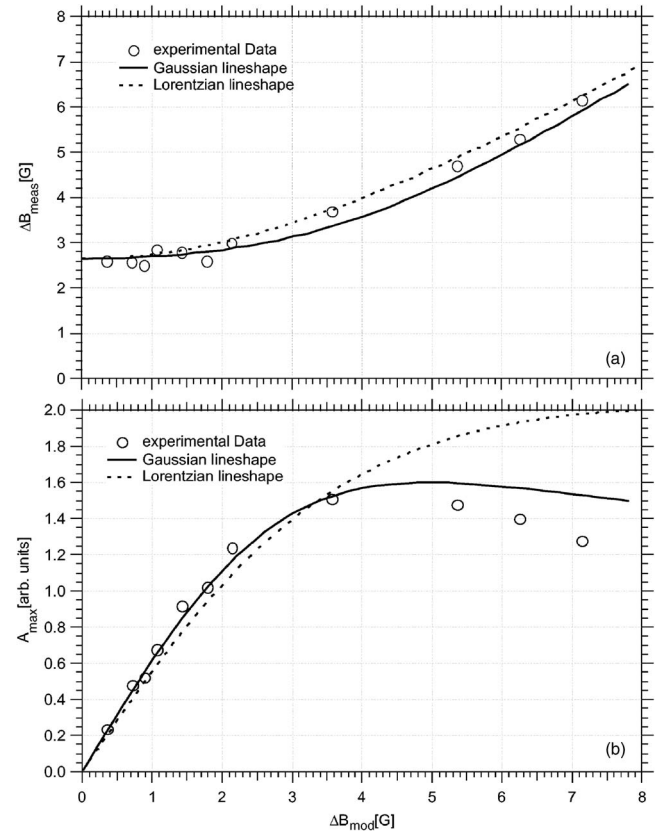


FIG. 3. Dependence (a) of the half linewidth ΔB_{meas} and (b) of the signal amplitude A_{max} as defined in Fig. 2 on the frequency modulation amplitude ΔB_{mod} in field units. Open symbols are experimental data points, theoretical calculations for a Gaussian and Lorentzian line shape are shown as a solid and dashed line, respectively.

tual line shape in a MRFM experiment it is more complicated due to the inhomogeneous tip field.¹⁵ This complicated line shape does not only affect the low field side of the resonance but also the high field side and needs to be taken into account in order to explain the influence of the modulation depth on the measured spectra. We also note that the linewidth measured in our experiments is somewhat larger than typically reported for conventional ESR measurements for DPPH,²⁶ which also suggests that the line is inhomogeneously broadened.

C. Frequency modulation at integer fractions of the cantilever frequency

Another interesting implication of Eq. (8) is that by modulating the microwave frequency at integer fractions of the cantilever frequency, i.e., $\omega_m = \omega_0/k$ ($k=1, 2, 3, \dots$), the cantilever response at its resonance frequency should reflect the k th derivative of the amplitude modulation response. For $k=1$ this has indeed been shown in the preceding paragraph. For $k=2$, i.e., $\omega_m = \omega_0/2$, the Fourier component at the cantilever frequency becomes

$$\left[\frac{1}{4} \frac{\partial^2 F}{\partial B^2} \Big|_{\bar{B}} \frac{\Delta\omega^2}{\gamma^2} + \frac{1}{48} \frac{\partial^4 F}{\partial B^4} \Big|_{\bar{B}} \frac{\Delta\omega^4}{\gamma^4} + \mathcal{O}(\Delta\omega^6) \right] \cos(\omega_0 t). \quad (11)$$

Thus to lowest order in $\Delta\omega$ the cantilever response of frequency modulation at half the cantilever resonance fre-

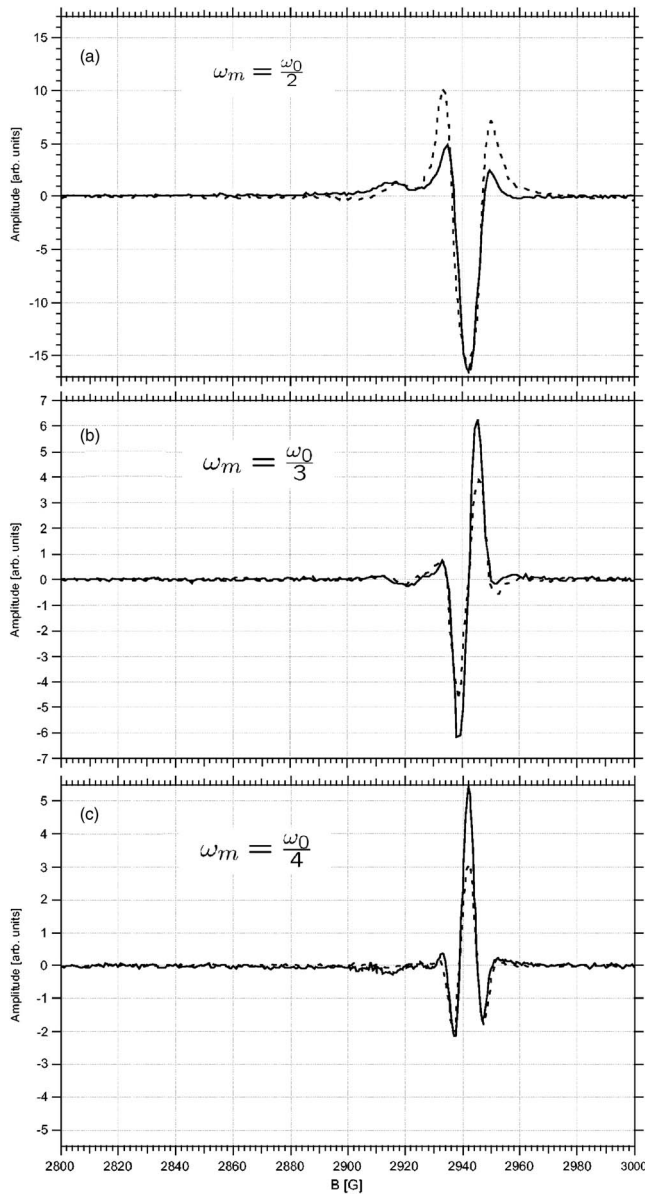


FIG. 4. Cantilever amplitude as a function of the applied magnetic field. Here the microwave field was frequency modulated with a modulation amplitude of $\Delta\omega/\gamma=5.4$ G at (a) half the cantilever frequency, (b) a third of the cantilever frequency, and (c) a fourth of the cantilever frequency. The signal at the cantilever frequency was detected using a lock-in amplifier. The solid lines in the graphs show the experimental data, while the dashed lines in (a), (b), and (c) are the numerical derivative of the data shown in Figs. 2, 4(a), and 4(b), respectively.

quency should be proportional to the second derivative of the amplitude modulation response. In Fig. 4(a) the cantilever amplitude measured using frequency modulation at $\omega_0/2$ is shown together with the second derivative of the amplitude modulation response, which was calculated as the numerical derivative of the frequency modulation response in Fig. 2. We note that second derivative curves of absorption spectra have been used in the past, see, for example, Refs. 23, 27, and 28. One advantage of using the second derivative signal rather than the first derivative signal is the fact that the location of the resonance is given by the minimum of the signal instead of the zero crossing, which relies on a proper background determination.

Similarly frequency modulation at a third of the cantilever frequency, i.e., $\omega_m=\omega_0/3$, the Fourier component at the cantilever frequency is

$$\left[\frac{1}{24} \frac{\partial^3 F}{\partial B^3} \bigg|_{\bar{B}} \frac{\Delta\omega^3}{\gamma^3} + \frac{1}{384} \frac{\partial^5 F}{\partial B^5} \bigg|_{\bar{B}} \frac{\Delta\omega^5}{\gamma^5} + \mathcal{O}(\Delta\omega^7) \right] \cos(\omega_0 t). \quad (12)$$

Therefore, the cantilever response in this case in lowest order of $\Delta\omega$ is proportional to the third derivative of the amplitude modulation response, as is shown in Fig. 4(b). In conventional spectroscopy experiments this has been previously observed by Rinehart *et al.*²³

Similar arguments hold for modulation at a quarter of the cantilever frequency, $\omega_m=\omega_0/4$; here the cantilever response in lowest order of $\Delta\omega$ is proportional to the fourth derivative of the amplitude modulation response, as shown in Fig. 4(c).

III. CONCLUSIONS

The use of low doped silicon cantilevers with a high coercivity SmCo particle glued to its end enables MRFM experiments using amplitude modulation of the microwave field with very low spurious coupling. Frequency modulation of the microwave field at the cantilever resonance frequency leads to a first derivative signal of the amplitude modulation response. The modulation depth in this case affects the experimentally observed linewidth and the signal amplitude, leading to an optimal modulation depth, maximizing the signal. Using frequency modulation of the microwave field at integer fractions of the cantilever frequency enables detection of higher order derivatives of the amplitude modulation signal. For a thin film of DPPH the high Q factor of the mechanical resonator enabled the detection up to the fourth derivative of the amplitude modulation response. The technique of modulating the microwave frequency at integer fractions of the cantilever frequency can be further extended to better conducting, i.e., highly doped, cantilevers to reduce the spurious coupling in MRFM experiments.

ACKNOWLEDGMENTS

The authors would like to thank C. Alexander for stimulating and fruitful discussions. Work at Los Alamos National Laboratory was supported by the U.S. Department of Energy. The work at Ohio State University was supported by the U.S. Department of Energy through Grant No. DE-FG02-03ER46054.

¹J. A. Sidles, Appl. Phys. Lett. **58**, 2854 (1991).

²O. Zuger, S. T. Hoen, C. S. Yannoni, and D. Rugar, J. Appl. Phys. **79**, 1881 (1996).

³A. Schaff and W. S. Veeman, Appl. Phys. Lett. **70**, 2598 (1997).

⁴B. J. Suh, P. C. Hammel, Z. Zhang, M. M. Midzor, M. L. Roukes, and J. R. Childress, J. Vac. Sci. Technol. B **16**, 2275 (1998).

⁵T. Mewes, J. Kim, D. V. Pelekhov, G. N. Kakazei, P. E. Wigen, S. Batra, and P. C. Hammel, Phys. Rev. B **74**, 144424 (2006).

⁶O. Zuger and D. Rugar, Appl. Phys. Lett. **63**, 2496 (1993).

⁷P. C. Hammel, Z. Zhang, G. J. Moore, and M. L. Roukes, J. Low Temp. Phys. **101**, 59 (1995).

⁸D. Rugar, R. Budakian, H. J. Mamin, and B. W. Chui, Nature (London) **430**, 329 (2004).

⁹K. J. Bruland, J. Krzystek, J. L. Garbini, and J. A. Sidles, Rev. Sci. In-

- strum. **66**, 2853 (1995).
- ¹⁰K. J. Bruland, W. M. Dougherty, J. L. Garbini, J. A. Sidles, and S. H. Chao, *Appl. Phys. Lett.* **73**, 3159 (1998).
- ¹¹Z. Zhang, M. L. Roukes, and P. C. Hammel, *J. Appl. Phys.* **80**, 6931 (1996).
- ¹²A. Suter, *Prog. Nucl. Magn. Reson. Spectrosc.* **45**, 239 (2004).
- ¹³K. Wago, D. Botkin, C. S. Yannoni, and D. Rugar, *Appl. Phys. Lett.* **72**, 2757 (1998).
- ¹⁴J. A. Marohn, R. Fainchtein, and D. D. Smith, *J. Appl. Phys.* **86**, 4619 (1999).
- ¹⁵A. Suter, D. Pelekhov, M. Roukes, and P. Hammel, *J. Magn. Reson.* **154**, 210 (2002).
- ¹⁶B. C. Stipe, H. J. Mamin, T. D. Stowe, T. W. Kenny, and D. Rugar, *Phys. Rev. Lett.* **87**, 096801 (2001).
- ¹⁷D. Rugar, H. J. Mamin, and P. Guethner, *Appl. Phys. Lett.* **55**, 2588 (1989).
- ¹⁸K. Wago, O. Zuger, J. Wegener, R. Kendrick, C. S. Yannoni, and D. Rugar, *Rev. Sci. Instrum.* **68**, 1823 (1997).
- ¹⁹K. Halbach, *Phys. Rev.* **119**, 1230 (1960).
- ²⁰O. Haworth and R. E. Richards, *Prog. Nucl. Magn. Reson. Spectrosc.* **1**, 1 (1966).
- ²¹C. Poole, *Electron Spin Resonance* (Dover, New York, 1983).
- ²²R. Karplus, *Phys. Rev.* **73**, 1027 (1948).
- ²³E. A. Rinehart, R. H. Kleen, and C. C. Lin, *J. Mol. Spectrosc.* **5**, 458 (1961).
- ²⁴H. Wahlquist, *J. Chem. Phys.* **35**, 1708 (1961).
- ²⁵G. W. Smith, *J. Appl. Phys.* **35**, 1217 (1964).
- ²⁶R. T. Weidner and C. A. Whitmer, *Phys. Rev.* **91**, 1279 (1953).
- ²⁷J. N. Herak and W. Gordy, *Proc. Natl. Acad. Sci. U.S.A.* **55**, 698 (1966).
- ²⁸J. Henry, L. Pugh, and J. C. Alexander, *J. Chem. Phys.* **66**, 726 (1977).